

Original Article

The Preliminary Study of Elucidating Structural Integrity of Microstructural White Matter Tract of Auditory Cortex in Noise-Induced Hearing Loss: An MRI-based Diffusion Tensor Imaging Study

Mohd Khairul Izamil Zolkefley^{a*}, Norhidayah Abdull^a, Rajeev Shamsuddin Perisamy^b, Muzaimi Mustapha^c, Daud Adam^d, Muhamad Ariff Muhamad Noordin^d

^aOccupational Safety and Health Program, Faculty of Industrial Sciences and Technology, Universiti Malaysia Pahang Al-Sultan Abdullah, Lebuhr Persiaran Tun Khalil Yaakob 26300, Kuantan Pahang, Malaysia

^bDepartment of Radiology, Sultan Ahmad Shah Medical Centre @IIUM, Jalan Sultan Ahmad Shah, Bandar Indera Mahkota, 25200 Kuantan, Pahang Malaysia

^cDepartment of Neurosciences, School of Medical Sciences, Universiti Sains Malaysia. 16150 Kubang Kerian Kota Bharu, Kelantan Malaysia

^dNational Institute of Occupational Safety and Health, Lot 1, Jalan 15/1, Seksyen 15, 43650 Bandar Baru Bangi, Selangor Malaysia.

*Corresponding author:

Article history

Received 07/03/2024

Accepted (Panel 1) 04/09/2024

ABSTRACT: *Introduction: Noise-induced hearing loss (NIHL) is considered the most common occupational disease in the world. Brain structural change is associated with hearing loss; however, there is limited information on association between white matter tract of auditory cortex and NIHL. Therefore, this study aimed to assess the role of diffusion tensor imaging (DTI) metrics in the evaluation of the microstructural integrity of the white matter tract of auditory cortex in NIHL. Methods: A total of nine patients with NIHL were recruited as participants. All the participants underwent magnetic resonance imaging brain scanning, and mean fractional anisotropy (FA) value from DTI analysis was extracted from the right and left areas of the auditory cortex. Correlation analysis was conducted between pure tone average data and mean FA value. Results: An inverse relationship was observed between mean FA and the degree of hearing loss, which was more significant in the left A1 area of auditory cortex ($p < 0.05$). Conclusion: The FA value is a valuable non-invasive biomarker in evaluating the subtle microstructural abnormalities of the white matter tract of auditory cortex in NIHL, and correlates well with hearing impairment.*

Keywords: *hearing loss, noise-induced hearing loss, diffusion tensor imaging, white matter*

All rights reserved.

1.0 INTRODUCTION

The complex hearing mechanism involves numerous ear elements that work together to transmit information to the brain. The auditory system is composed of central regions (cochlear nuclei in the medulla oblongata, superior olivary nuclei, and lateral lemniscus in the pons; inferior colliculus in the midbrain; medial geniculate nuclei in the thalamus; and auditory cortex in the superior temporal Heschl's gyrus) and peripheral structures (external, middle, and inner ear). Most auditory fibres decussate contralaterally to the opposing superior olive in the trapezoidal body region (Lee & Sherman, 2011).

Hearing loss is the fourth leading cause of disability. It impairs communication, with adverse effects on relationships with others (Cunningham & Tucci, 2017). Hearing loss is defined based on the audiometric threshold. The World Health Organization has classified hearing impairment according to pure-tone audiometry in the better hearing ear as: (1) no impairment [≤ 25 dB hearing threshold level (HL)]; (2) slight impairment (26–40 dB HL); (3) moderate impairment (41–60 dB HL); (4) severe impairment (61–80 dB HL); and (5) profound impairment (≥ 81 dB HL; Olusanya, Davis, & Hoffman, 2019). Peripheral hearing loss is categorised as conductive or sensorineural. Sensorineural hearing loss (SNHL) results from malfunction of the cochlea or spiral ganglion, whereas conductive hearing loss results from damage to the outer or middle ear (Cunningham & Tucci, 2017). Noise-induced hearing loss (NIHL) is an SNHL that affects the hair cells of the inner ear and has been used by clinicians to refer to either a malfunctioning inner ear or a retro-cochlear problem affecting the canalicular VIII cranial nerve and cerebellopontine angle, or involving the higher (central) auditory nuclei and neural tracts. To develop a treatment plan that can assist in preventing or delaying the total loss of auditory function, it is important to understand the pathophysiology of hearing loss (Verbist, 2012).

In recent years, advanced magnetic resonance spectroscopy, magnetic resonance morphometry, functional magnetic resonance imaging (fMRI), and diffusion tensor imaging (DTI) have revealed microstructural and functional alterations to the auditory system. For example, magnetic resonance spectroscopy simplifies the display of changes in the concentrations and contents of certain metabolites in the central nervous system. In addition, fMRI has shown that individuals with idiopathic SNHL and healthy individuals have different levels of central auditory circuit activation (Ouda, Profant, & Syka, 2015). DTI has become a common tool for research in recent years for examining the microstructural integrity linked to white matter disorders (de Figueiredo, Borgonovi, & Doring, 2011; Yang et al., 2023; Zhang et al., 2022). This is based on the concept that water diffusion is restricted perpendicular to the axis of the axons, causing anisotropy (Aung, Mar, & Benzinger, 2013). Organised packed axonal tracts, overlying sheets of myelin, microtubules, and neurofilaments represent the physical barriers that impose directionality on water movement in the tissues of the central nervous system. Anisotropic diffusion can be distinguished using a sensitive and non-invasive quantitative method by calculating the diffusion tensor indices mean diffusivity and fractional anisotropy (FA) for every voxel (Kerkelä et al., 2021). The FA value, as observed in healthy brain tissues, is a scalar number between 0 (indicating unrestricted diffusion in all directions) and 1 (indicating unrestricted diffusion in only one direction). Therefore, decreased FA is a sensitive indicator of the loss of white matter integrity. Changes in tissue density, damage to white matter fibres, or alterations in the overlying myelin sheath can influence these indices by affecting the directionality of water motion (Huang et al., 2015).

To date, there is a lack of studies using DTI to evaluate the microstructural alterations in the brain and their associations with NIHL in employees who have been exposed to high noise levels at work for an extended period of time. Therefore, this study aimed to examine how NIHL affects anatomical alterations in the microstructure of the brain as measured using DTI metric–FA parameters). In this study, we focused on the area surrounding the primary auditory cortex. This study aimed to evaluate subtle and microstructural changes in DTI metrics–FA within the auditory cortex and correlate them with hearing threshold levels of pure tone average data in the participants. Hence, this study assessed the potential of brain information as a novel biomarker of great importance for the early detection, diagnosis, and assessment of the severity and progression of NIHL as well as its prognosis and expected response to preventive and therapeutic interventions.

2.0 METHOD

2.1 Patients

This study was approved by the Research Ethics Committee of International Islamic University Malaysia, and informed consent was obtained from each patient prior to examination. The present study included nine gender-matched male patients with bilateral NIHL. All participants enrolled in the current study had normal peripheral and central auditory circuits, as determined by conventional MRI studies. The participants had no history of brain surgery, trauma, infection, or ototoxic medication use.

All participants underwent a comprehensive audiological history taking and otoscopic examination, and pure-tone average data for each participant were obtained. Hearing loss ranged from mild to severe (30–90 dB).

2.2 MRI

All MRI images were acquired using a Siemens 3-Tesla MR scanner. Before DTI acquisition, non-contrast conventional MR was performed to exclude gross abnormalities in the peripheral and central auditory pathways. The MR imaging protocols included the following sequences: 1) The T1 parameters were TE/TR = 10/678 msec; reconstruction matrix = 512 x 512 x 40; field of view = 230 mm; voxel size = 0.45 x 0.45; slice spacing = 1.0 mm; slice thickness = 2.5 mm; and flip angle = 70 degree. 2) T2 parameters were TE/TR = 80/3000 msec; reconstruction matrix = 512 x 512 x 24; field of view = 230 mm; voxel size = 0.45 x 0.45; slice spacing = 1.0 mm; slice thickness = 2.5 mm; and flip angle = 90°. 3) FLAIR parameters were TE/TR/TI = 125/11000/2800 msec; reconstruction matrix = 512 x 512 x 40; field of view = 230 mm; voxel size = 0.45 x 0.45; slice spacing = 1.0 mm; slice thickness = 5.0 mm; and flip angle = 90°.

2.3 DTI Acquisition

The DTI parameters were set as follows: repetition time = 7649 ms, echo time = 72 ms, flip angle = 90°, field of view = 240 mm, matrix = 96 x 96, section thickness = 2.5 mm, section gap = 0 mm, number of excitations = 1.0, and acquisition time = 4 min and 28 s. Diffusion-weighting gradients were applied along 32 non-collinear directions using the electrostatic repulsion model (b0 = 0, 2 images and b1 = 1000 s/mm, 32 images).

2.4 DTI data processing

Diffusion-imaging data were reconstructed using the DTI approach with the combined use of MRI Converter version 2.1.0 and DSI Studio software (<http://dsi-studio.labsolver.org/>). First, the Digital Imaging and Communications in Medicine data of each participant were loaded into the MRI Converter to convert it into NIfTI file format (.dcm to .nii) before opening them in DSI Studio. The automated registration of the DTI data was done to eliminate distortion artefacts. Then, the '.src' file was created, reconstructed and '.fib' data were obtained to track the fibres and tractography, followed by the acquisition of the mean FA value. The regions of interest (ROIs) assessed were those in the cortical parcellation of the auditory network (Kuiper et al., 2020): A1, A4, A5, LBelt, MBelt, and PBelt (Figure 1). The ROIs from both hemispheres were localised using semi-automated delimitation. This technique was used by combining the automated identification of the ROI (a validated atlas of John Hopkins University white matter labels atlas was used as a template) with a manual, interactive selection, and modification by the user (de Haan, Clas, Juenger, Wilke, & Karnath, 2015). The mean FA values of each region from both hemispheres were extracted from the ROIs for further analysis.

2.5 Statistical Analysis

Data were analysed using the IBM SPSS software package version 22.0. Quantitative data were described by calculating the means and standard deviations of non-parametric data because of the small number of samples with p-values < 0.05, which were considered statistically significant. The Spearman correlation test was used to determine the correlation between changes in the FA measures and hearing loss levels (pure tone average data) in NIHL.

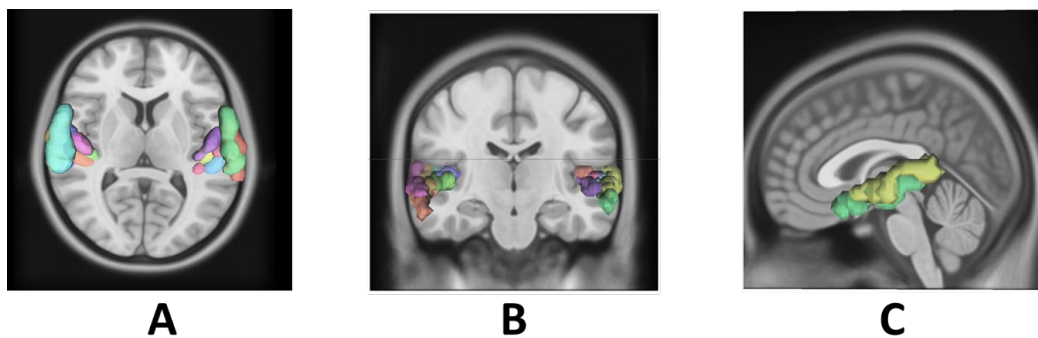


Figure 1: Acquisition of region of interest in the cortical parcellation of the auditory cortex: left and right A1, A4, A5, LBelt, MBelt, PBelt. The view from different axes: A) axial, B) coronal, C) sagittal section.

3.0 RESULTS

Table 1 summarizes the mean and standard deviation of participants ages, pure tone average data for the right and left ears, and FA values measured in six regions: A1, A4, A5, LBelt, MBelt, and PBelt.

Table 1. Mean and standard deviation of participants’ age, right and left pure tone average data^a, and fractional anisotropy values measured in six regions: A1, A4, A5, LBelt, MBelt, and PBelt

Variables	Mean ± SD values (n = 9)
Age	45 ± 6.1
Right pure tone average (dB) ^a	38.5 ± 13.5
Left pure tone average (dB) ^a	41.5 ± 13.3
FA values measured in different regions of auditory cortex	
<i>Right side</i>	
A1	0.174 ± 0.022
A4	0.096 ± 0.015
A5	0.106 ± 0.015
LBelt	0.180 ± 0.033
MBelt	0.211 ± 0.027
PBelt	0.179 ± 0.031
<i>Left side</i>	
A1	0.171 ± 0.031
A4	0.091 ± 0.017
A5	0.103 ± 0.008
LBelt	0.192 ± 0.029
MBelt	0.218 ± 0.023
PBelt	0.166 ± 0.023

^a Pure Tone Average = (0.5 Khz + 1 Khz + 2 Khz + 4khz)/4.

The correlations between the mean FA values in the six regions and the measured hearing levels (pure tone average data) are summarised in Table 2. A significant inverse relationship was found between the left mean FA value of the A1 region and both the right ($p = 0.009$, $r = -0.807$) and left ($p = 0.03$, $r = -0.717$) pure tone average data, whereas no significant correlation was found between the mean FA values in other regions and the severity of hearing impairment.

Table 2. Correlation analysis between mean fractional aAnisotropy and severity of sensorineural hearing impairment (pure tone average)

Regions in auditory cortex	Right pure tone average		Left pure tone average	
	<i>p</i> -value	<i>r</i> -value	<i>p</i> -value	<i>r</i> -value
<i>Right side</i>				
A1	0.796	0.101	0.932	0.033
A4	0.456	0.286	0.244	0.433
A5	0.983	0.008	0.865	0.067
LBelt	0.682	-0.160	0.732	-0.133
MBelt	0.332	-0.367	0.557	-0.227
PBelt	0.406	-0.317	0.260	-0.420
<i>Left side</i>				
A1	0.009**	-0.807	0.030*	-0.717
A4	0.364	-0.345	0.286	-0.400
A5	0.079	-0.613	0.088	-0.600
LBelt	0.949	0.025	0.688	0.167
MBelt	0.415	0.311	0.356	0.350
PBelt	0.250	-0.429	0.308	-0.383

*Correlation is significant at the 0.05 level (two-tailed).
**Correlation is significant at the 0.01 level (two-tailed).

4.0 DISCUSSION

Our preliminary results revealed a significant negative correlation between the mean FA value of the left A1 region and the left and right pure tone average data. It is anticipated that hearing loss with a dominant effect on the contralateral side may affect both the ipsilateral and contralateral auditory neural pathways because of the early and numerous decussations of the auditory nerve system beginning at the cochlear nucleus level (Tae, Yakunina, Kim, Kim, & Nam, 2014). However, the cause of these asymmetries in humans is either difficult to identify or extremely difficult to address because of the widespread corticofugal effects on the auditory system. It makes no difference as to whether the laterality of function results from central or peripheral influences, as it is crucial to comprehend the nature of minute variations in the ear structure. For instance, adult males typically have better audiometric hearing thresholds in the right ear than in the left ear; however, women are known to have more symmetric hearing sensitivity. Better hearing in the right ear of adults may be related to another asymmetry: greater susceptibility of the left ear to NIHL (Pirilä, Jounio-Ervasti, & Sorri, 1992).

Because the ventral division of the medial geniculate complex provides point-to-point input to the primary auditory cortex (A1), which is situated on the superior temporal gyrus in the temporal lobe, it has an accurate tonotopic map that spans a large range of sound frequencies. This explains the strong association between the A1 region and pure tone average data (which comprise a range of sound frequencies) in our study. Similar to the main visual cortex (V1) and primary somatic sensory cortex (S1) having topographical maps of their respective sensory epithelia, the primary auditory cortex (A1) has a topographical map of the cochlea (Alloway, 2001). However, unlike the visual and somatic sensory systems, the cochlea had already decomposed acoustic stimuli such that they were arrayed tonotopically along the length of the basilar membrane. As a result, A1 and most of the ascending auditory structures between the cochlea and cortex were thought to include a tonotopic map, which explains their close association with pure tone average values computed from various sound frequency ranges. However, because the belt sections of the medial geniculate complex receive more diffuse input, the belt areas of the auditory cortex are less accurate in their tonotopic organisation (Brewer & Barton, 2016).

Our findings showed an inverse relationship between the mean FA value in the A1 region and pure-tone average data, suggesting a reduction in mean FA with hearing loss. Previous research on patients with SNHL revealed decreased brain activity in several cortical and subcortical regions, such as the inferior colliculus and temporal gyrus, as well as a decrease in the amount of cortical grey matter (Kim, Heo, Kim, Kim, & Oh, 2018). DTI research in neurology has yielded promising results, indicating the usefulness of this novel radiological approach. As auditory deprivation results in inadequate myelination, hearing loss can produce cortical and subcortical microstructural alterations in numerous auditory neurological systems (Kim et al., 2018). Diffusion tensor metrics offer quantitative information on the myelination status and microstructural integrity of the central auditory circuit in auditory diseases. They also provide important prognostic information regarding progressive hearing loss (Tarabichi et al., 2018). Owing to decreased functional activity in the auditory pathway, a demyelination process may be present. This may be caused by increased water diffusivity across the neural fibre tracts. In our investigation, the principal auditory area (the 'A' area) had lower mean FA values than the belt areas. Because the primary auditory area is a convergence site for inputs from various caudal auditory nuclei, it may be more susceptible to neuronal damage than the belt areas. This could be explained by the primary anatomical location of the auditory area in the central auditory circuit, and consequently, greater myelin degeneration (Lin et al., 2008). FA may be regarded as a useful biological indicator of the degree of hearing impairment, based on earlier findings that showed an apparent linear association between decreased FA values and audiometric hearing loss (Kim et al., 2018). Similarly,, the current study showed that FA measures were inversely correlated with hearing loss.

Our preliminary study has some limitations. The primary limitation was the small population of the NIHL group, which hindered the stratification of patients according to the severity of hearing loss. In addition, only six regions of the auditory network were investigated in this study. Further studies investigating other regions of the auditory tract are essential to determine their roles in hearing impairments. Another limitation was the age of the participants, which was not restricted; thus, the results may have included age-related brain degeneration. Therefore, a larger subject pool is necessary to derive detailed prognostic predictions for different age groups. Furthermore, we did not measure the long-term effects of NIHL on the brain, and longitudinal studies are needed to explore the changes in brain imaging and NIHL. In addition, the absence of reproducibility of FA correlations with repeated pure-tone average data in a longitudinal study may indicate a deficiency in the correlation analysis.

6.0 CONCLUSION

A decline in FA values can be used to reflect microstructural abnormalities of the central auditory tract in patients with NIHL and is correlated with the degree of hearing impairment in the auditory cortex. Although the correlation analysis data should be interpreted cautiously owing to the small sample size and statistical power, we propose that information about central auditory pathway integrity should be included as a potential novel neurological biomarker for early detection, diagnosis, and assessment of the severity and progression of NIHL.

ACKNOWLEDGEMENT

This work was supported by the National Institute of Occupational Safety and Health (NIOSH) research grant [03.16/03/NIHL(E)/2023/01; UMP grant number: RDU230702]. Special gratitude is given to all authors for their expertise and assistance in completing the project and writing the manuscript.

REFERENCES

- Alloway, K. (2001). Neuroscience Dale Purves George J. Augustine David Fitzpatrick Lawrence C. Katz Anthony-Samuel LaMantia James O. McNamara S. Mark Williams. *Quarterly Review of Biology - QUART REV BIOL*, 76. doi:10.1086/420640
- Aung, W. Y., Mar, S., & Benzinger, T. L. (2013). Diffusion tensor MRI as a biomarker in axonal and myelin damage. *Imaging Med*, 5(5), 427-440. doi:10.2217/iim.13.49
- Brewer, A. A., & Barton, B. (2016). Maps of the Auditory Cortex. *Annu Rev Neurosci*, 39, 385-407. doi:10.1146/annurev-neuro-070815-014045
- Cunningham, L. L., & Tucci, D. L. (2017). Hearing Loss in Adults. *N Engl J Med*, 377(25), 2465-2473. doi:10.1056/NEJMra1616601
- de Figueiredo, E. H. M. S. G., Borgonovi, A. F. N. G., & Doring, T. M. (2011). Basic Concepts of MR Imaging, Diffusion MR Imaging, and Diffusion Tensor Imaging. *Magn Reson Imaging Clin N Am*, 19(1), 1-22. doi:https://doi.org/10.1016/j.mric.2010.10.005
- de Haan, B., Clas, P., Juenger, H., Wilke, M., & Karnath, H. O. (2015). Fast semi-automated lesion demarcation in stroke. *Neuroimage Clin*, 9, 69-74. doi:10.1016/j.nicl.2015.06.013
- Huang, L., Zheng, W., Wu, C., Wei, X., Wu, X., Wang, Y., & Zheng, H. (2015). Diffusion Tensor Imaging of the Auditory Neural Pathway for Clinical Outcome of Cochlear Implantation in Pediatric Congenital Sensorineural Hearing Loss Patients. *PLOS ONE*, 10(10), e0140643. doi:10.1371/journal.pone.0140643
- Kerkelä, L., Nery, F., Callaghan, R., Zhou, F., Gyori, N. G., Szczepankiewicz, F., . . . Clark, C. A. (2021). Comparative analysis of signal models for microscopic fractional anisotropy estimation using q-space trajectory encoding. *NeuroImage*, 242, 118445. doi:10.1016/j.neuroimage.2021.118445
- Kim, S. Y., Heo, H., Kim, D. H., Kim, H. J., & Oh, S. H. (2018). Neural Plastic Changes in the Subcortical Auditory Neural Pathway after Single-Sided Deafness in Adult Mice: A MEMRI Study. *Biomed Res Int*, 2018, 8624745. doi:10.1155/2018/8624745
- Kuiper, J. J., Lin, Y.-H., Young, I. M., Bai, M. Y., Briggs, R. G., Tanglay, O., . . . Sughrue, M. E. (2020). A parcellation-based model of the auditory network. *Hearing Research*, 396, 108078. doi:https://doi.org/10.1016/j.heares.2020.108078
- Lee, C. C., & Sherman, S. M. (2011). On the classification of pathways in the auditory midbrain, thalamus, and cortex. *Hear Res*, 276(1-2), 79-87. doi:10.1016/j.heares.2010.12.012
- Lin, Y., Wang, J., Wu, C., Wai, Y., Yu, J., & Ng, S. (2008). Diffusion tensor imaging of the auditory pathway in sensorineural hearing loss: changes in radial diffusivity and diffusion anisotropy. *J Magn Reson Imaging*, 28(3), 598-603. doi:10.1002/jmri.21464
- Olusanya, B. O., Davis, A. C., & Hoffman, H. J. (2019). Hearing loss grades and the International classification of functioning, disability and health. *Bull World Health Organ*, 97(10), 725-728. doi:10.2471/blt.19.230367
- Ouda, L., Profant, O., & Syka, J. (2015). Age-related changes in the central auditory system. *Cell Tissue Res*, 361(1), 337-358. doi:10.1007/s00441-014-2107-2
- Pirilä, T., Jounio-Ervasti, K., & Sorri, M. (1992). Left-right asymmetries in hearing threshold levels in three age groups of a random population. *Audiology*, 31(3), 150-161. doi:10.3109/00206099209072910
- Tae, W. S., Yakunina, N., Kim, T. S., Kim, S. S., & Nam, E. C. (2014). Activation of auditory white matter tracts as revealed by functional magnetic resonance imaging. *Neuroradiology*, 56(7), 597-605. doi:10.1007/s00234-014-1362-y
- Tarabichi, O., Kozin, E. D., Kanumuri, V. V., Barber, S., Ghosh, S., Sitek, K. R., . . . Lee, D. J. (2018). Diffusion Tensor Imaging of Central Auditory Pathways in Patients with Sensorineural Hearing Loss: A Systematic Review. *Otolaryngol Head Neck Surg*, 158(3), 432-442. doi:10.1177/0194599817739838
- Verbist, B. M. (2012). Imaging of sensorineural hearing loss: a pattern-based approach to diseases of the inner ear and cerebellopontine angle. *Insights Imaging*, 3(2), 139-153. doi:10.1007/s13244-011-0134-z
- Yang, Z., Xiao, S., Su, T., Gong, J., Qi, Z., Chen, G., . . . Wang, Y. (2023). A multimodal meta-analysis of regional functional and structural brain abnormalities in obsessive-compulsive disorder. *Eur Arch Psychiatry Clin Neurosci*. doi:10.1007/s00406-023-01594-x
- Zhang, X., Suo, X., Yang, X., Lai, H., Pan, N., He, M., . . . Gong, Q. (2022). Structural and functional deficits and couplings in the cortico-striato-thalamo-cerebellar circuitry in social anxiety disorder. *Translational Psychiatry*, 12(1), 26. doi:10.1038/s41398-022-01791-7